

Cystic Lesions of the Gastrointestinal Tract: Multimodality Imaging with Pathologic Correlations

Jongmee Lee, MD¹
Cheol Min Park, MD¹
Kyeong Ah Kim, MD¹
Chang Hee Lee, MD¹
Jae Woong Choi, MD¹
Bong Kyung Shin, MD²
Soon Jin Lee, MD³
Dongil Choi, MD³
Kee-Taek Jang, MD⁴

The cystic lesions of the gastrointestinal (GI) tract demonstrate the various pathologic findings. Some lesions may present a diagnostic challenge because of non-specific imaging features; however, other lesions are easily diagnosed using characteristic radiologic features and anatomic locations. Cystic masses from the GI tract can be divided into several categories: congenital lesions, neoplastic lesions (cystic neoplasms, cystic degeneration of solid neoplasms), and other miscellaneous lesions. In this pictorial review, we describe the pathologic findings of various cystic lesions of the GI tract as well as the radiologic features of GI cystic lesions from several imaging modalities including a barium study, transabdominal ultrasound (US), computed tomography (CT), and magnetic resonance (MR) imaging.

Index terms:

Cystic lesions
Gastrointestinal tract
Barium study
Ultrasound (US)
Computed tomography (CT)
Magnetic resonance (MR)

DOI:10.3348/kjr.2010.11.4.457

Korean J Radiol 2010; 11: 457-468

Received October 26, 2009; accepted after revision March 24, 2010.

Departments of ¹Radiology, ²Pathology, Korea University Guro Hospital, Korea University College of Medicine, Seoul 152-703, Korea; ³Department of Radiology and Center for Imaging Science, ⁴Department of Pathology, Samsung Medical Center, Sungkyunkwan University School of Medicine, Seoul 135-710, Korea

Address reprint requests to:

Jongmee Lee, MD, Department of Radiology, Korea University Guro Hospital, Korea University College of Medicine, 80 Guro-dong, Guro-gu, Seoul 152-703, Korea.
Tel. (822) 2626-1338
Fax. (822) 2626-1379
e-mail: jongmee.lee@gmail.com

Cystic lesions of the gastrointestinal (GI) tract rarely occur and often demonstrate various pathologic findings. These lesions can be divided into several categories: congenital lesions, neoplastic lesions, and miscellaneous lesions (Table 1). Most of the cystic masses of the GI tract are discovered incidentally and usually appear as submucosal lesions. Patients can present with a variety of symptoms, including abdominal pain, bowel obstruction, perforation, intussusception, intestinal bleeding, and associated malignancy. Histologically, most of the cystic lesions of the GI tract are benign; however, some represent cystic changes in malignant tumors or potentially malignant. A number of imaging modalities, such as plain abdominal radiograph, barium study, transabdominal ultrasonography (US), computed tomography (CT), and magnetic resonance (MR) imaging, have been used to differentiate among cystic lesions. Although the roles of radiologic imaging modalities are limited due to a substantial overlap in radiologic findings, some cystic lesions have predominant or specific radiologic features. When these features are coupled with the anatomic location of a lesion, a correct diagnosis can often be inferred.

Herein, we describe and illustrate the multimodality imaging features of cystic lesions of the GI tract, and correlate these features with pathologic findings in order to suggest a specific diagnosis or to substantially narrow the differential diagnosis using the imaging appearance and anatomic location of the lesion.

CONGENITAL LESIONS

Duplication Cyst

Duplication cysts of the GI tract are rare congenital anomalies that most commonly affects the ileum, followed by the esophagus, large bowel, and jejunum (1, 2). Duplication cysts of the stomach (Fig. 1) and duodenum (Fig. 2) are uncommon,

comprising only 5–7% of all intestinal duplications (1). The three diagnostic criteria for duplication cysts include the presence of an intimate attachment to the GI tract, a layer of smooth muscle in the wall, and an epithelial lining resembling some part of the GI tract (1). The cysts become incorporated into the bowel wall and share a common blood supply with the parent bowel. Duplication cysts may also contain heterotopic tissues, including gastric mucosa, pancreas (Fig. 1), lymphoid tissue, and respiratory epithelium (1, 3). The clinical manifestations of duplication cysts depend on the location, size, and mucosal pattern. GI bleeding or perforation is especially likely if duplications contain ectopic gastric mucosa, which occurs in 20–50% of duplications or ectopic pancreatic tissue (1, 2).

A plain abdominal radiograph may help detect a soft tissue mass, or sometimes a curvilinear calcification of the cystic wall (1). A barium study would divulge a polypoid submucosal mass (Fig. 1) or indentation of the GI tract by an extrinsic mass. If the duplications communicate with the lumen, the spherical or tubular structures filled with barium would appear to be adjacent to the GI tract. The diagnosis of duplications is easily achieved when the typical sonographic findings with an inner echogenic mucosa and an outer hypoechoic muscle layer are demonstrated within the cyst on transabdominal US (4). If duplication cysts become infected or hemorrhage occurs in the cyst, echogenic debris may be detected (Fig. 2). The CT findings of duplications usually include a large, well-circumscribed, spherical (Fig. 1), or tubular (Fig. 2) cystic mass. Rarely,

duplication cysts co-exist with wall calcifications or enterocoliths. On MR imaging, duplications are seen as well-circumscribed, homogeneous, hypointense masses on a T1-weighted image with a high signal intensity, accompanied by various internal signals due to associated hemorrhage or mucous secretion on a T2-weighted image (Fig. 2). The thin cyst wall shows slight enhancement with contrast.

Heterotopic Pancreas

A heterotopic pancreas is characterized by the presence of normally developed pancreatic tissue outside its usual anatomic location without any anatomic or vascular continuity. A heterotopic pancreas occurs throughout the GI tract, most commonly in the stomach, followed by the duodenum and jejunum (5). In the stomach, a heterotopic pancreas tends to be located along the greater curvature of the gastric antrum within 6 cm of the pyloric canal; whereas, in the duodenum, it tends to be located in the proximal duodenum between the duodenal bulb and the ampulla of Vater (6, 7). Histologically, a heterotopic pancreas is composed of all of the pancreatic elements, including acini, islets of Langerhans, and ductal structures (Fig. 3), and is usually located in the submucosa. Cyst formation in a heterotopic pancreas is caused by secondary changes in the pancreatic tissue, including pseudocyst formation or cystic dystrophy (8). A heterotopic pancreas may result in epigastric pain or upper GI bleeding from irritation or ulceration of the adjacent mucosa by pancreatic secretions.

A heterotopic pancreas, identified by a barium study, has been described as a solitary, sharply-defined submucosal nodule. In rare cases, a central umbilication may be visualized, resulting from the reflux of barium into the rudimentary duct of the heterotopic pancreas. The CT findings of a heterotopic pancreas cover a diverse spectrum, including a unilocular cystic lesion (Fig. 3), multiple cysts, and a solid mass with contrast enhancement (5, 7, 9). On CT, a heterotopic pancreas shows a well-defined, oval, submucosal mass with smooth margins. Small hypodense areas may exist within the lesions, suggesting dilated ducts within the heterotopic pancreas. MR images show cystic lesions in a thickened wall of the GI tract (8).

CYSTIC NEOPLASMS

Appendix Mucocele

Appendix mucoceles are dilatations of the appendix caused by an abnormal accumulation of mucus within the lumen. They have been identified in only 0.2–0.3% of appendectomy specimens on pathologic evaluation (10). The gross appearance of an appendix mucocele on pathologic evalua-

Table 1. Classification of Cystic Lesions of Gastrointestinal Tract

Lesions	Preferential Locations
CONGENITAL LESIONS	
Duplication cyst	ileum, esophagus, colon
Heterotopic pancreas	stomach (usually antrum), duodenum
Tailgut cyst	retrorectal/presacral space
NEOPLASTIC LESIONS	
Cystic Neoplasms	
Lymphangioma	colon, duodenum
Teratoma	cecum, rectosigmoid colon
Cystic Degeneration of Solid Neoplasms	
Schwannoma	stomach
Gastrointestinal stromal tumor	stomach, small bowel
Adenocarcinoma	colon, rectum
MISCELLANEOUS LESIONS	
Brunner's gland hyperplasia	duodenum
Gastritis cystica profunda	stomach (body and antrum)
Colitis cystica profunda	rectum, sigmoid colon
Intramural pseudocyst	duodenum (second portion)

Cystic Lesions of GI Tract

tion is one of a tubular or spherical mucus-filled mass (Fig. 4), which is divided into four categories according to the features of the epithelium: retention mucocele, mucinous cystadenoma, mucinous adenocarcinoma, and mucinous tumors of uncertain malignant potential. Retention mucoceles are usually unilocular and lined by flattened, atrophic epithelium. Mucinous cystadenomas are circumferentially lined by neoplastic mucinous epithelium that replaces the normal epithelium (Fig. 4). Clinical manifestations of mucinous cystadenomas include a palpable abdominal mass, right lower abdominal pain, intussusception, gastrointestinal bleeding, right ureteral obstruction, and increasing abdominal girth of pseudomyxoma peritonei, which is characterized by the intraperitoneal accumulation of mucin (11, 12).

A plain abdominal radiograph may show a soft-tissue mass in the right lower quadrant of the abdomen. In addition, the presence of a curvilinear wall calcification strongly supports the diagnosis of an appendix mucocele

(Fig. 4). However, this finding is only seen in < 50% of cases (11). Transabdominal US usually reveals a unilocular, ovoid, anechoic mass in the region of the appendix (Fig. 4). The intraluminal echogenicity can be variable, including numerous, fine echo spots or soft echogenic masses according to acoustic interfaces produced by the mucin (13).

When a mural calcification is present, sonography shows a highly echogenic wall with posterior shadowing (Fig. 4). CT can effectively demonstrate the anatomic relationship between the cystic mass and the cecum and the typical CT findings of an appendix mucocele are a round or tubular cystic mass with thin and enhancing walls in the appendiceal region (Fig. 4). Dystrophic calcification may be present in the wall of the mucocele (Fig. 4). On CT, pseudomyxoma peritonei appears as a low-attenuation substance in the abdomen, simulating ascites. MR imaging of an appendix mucocele reveals the cystic nature of the lesion, whereas a mural calcification is less apparent on MR imaging (12).

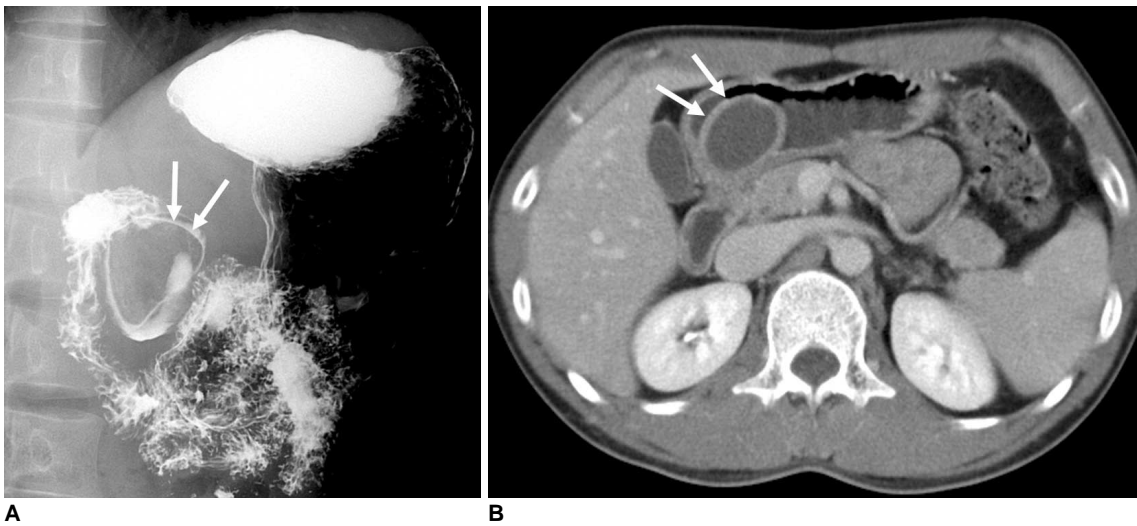


Fig. 1. Gastric duplication cyst in 29-year-old man.

A. Upper gastrointestinal series shows oval polypoid mass (arrows) with smooth border in gastric antrum.

B. Contrast-enhanced CT scan demonstrates oval cystic lesion with evenly enhancing wall (arrows) in posterior wall of gastric antrum.

C. Photomicrograph demonstrates normal gastric mucosa (arrows) and smooth muscle layer. Heterotopic pancreatic tissue island (asterisk) is shown in submucosal layer (Hematoxylin & Eosin stain, $\times 100$).

Lymphangioma

Lymphangiomas are uncommon benign tumors of the GI tract consisting of several expanded lymphatics in the submucosal layer. They are thought to arise from sequestered lymphatic tissue that fails to communicate with the normal lymphatic system. In general, lymphangiomas are solitary lesions; however, they can be present in multiples. GI lymphangiomas occur most frequently in the colon, followed by the duodenum and stomach (11). Grossly, lymphangiomas appear as round or oval translucent lesions covered by smooth mucosa. The cut surface of the lesion reveals a multicystic appearance that exudes a clear yellow or milky fluid (Fig. 5). Histologically, lymphangiomas are characterized by a localized proliferation of dilated lymphatic channels lined by benign-appearing endothelial cells (Fig. 5). Occasionally, lymphangiomas are large enough to cause obstructive symptoms or intussusception (11, 14). On endoscopy, GI lymphangiomas appear as soft, blue-tinged, submucosal masses

(Fig. 5) with distended mucosal vessels. The shape of the mass is easily altered when pressure is applied.

A barium study demonstrates sharply demarcated submucosal masses that are indistinguishable from other mesenchymal tumors (Fig. 5). Because of their cystic nature, these lesions may be pliable on fluoroscopy and the shape may easily change in response to peristaltic movement and manual compression (15). On CT, GI lymphangiomas appear as round submucosal masses with homogeneous low attenuation and a well-demarcated, smooth margin (Fig. 5). The lesion may be unilocular or multicystic. A CT scan may show multiple sporadic calcifications when multiple lymphangiomas are present (14).

CYSTIC DEGENERATION OF SOLID TUMORS

Occasionally, some types of solid neoplasms (i.e., gastrointestinal stromal tumors, neurogenic tumors, and

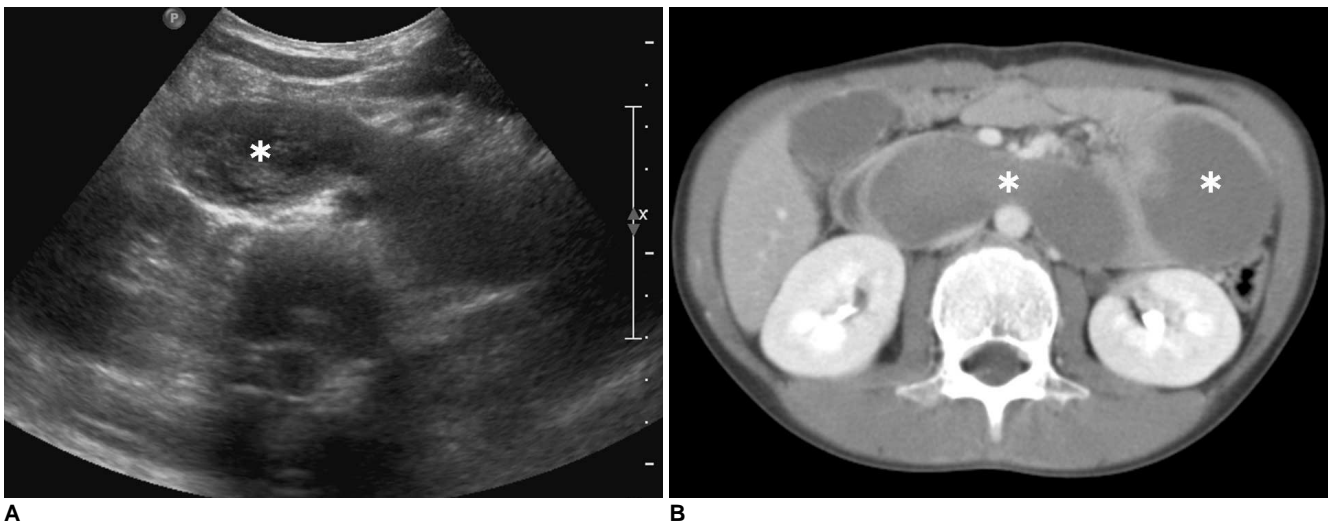


Fig. 2. Duodenal duplication cyst in 9-year-old boy. **A.** Transabdominal ultrasound shows tubular cystic lesion with internal debris (asterisk) in anterior aspect of both kidneys. **B.** CT scan demonstrates tubular cystic lesion (asterisks) along duodenum and extending toward jejunum. Cystic lesion showed presence of fluid with higher attenuation than water, suggestive of hemorrhage on precontrast CT scan (not shown). **C.** T2-weighted MR imaging shows well-circumscribed mass (asterisks) with slightly high signal intensity in abdomen.

adenocarcinomas) of the GI tract appear to be cystic. Cystic changes in a solid tumor can result from central necrosis of a large mass due to an inadequate blood supply. Other suggested mechanisms of cyst formation include liquefaction of an intratumoral hemorrhage or a treatment effect of chemotherapy.

It is difficult to radiologically discriminate between complex cystic lesions and cystic changes of solid tumors of the GI tract. Some radiologic features are more favorable for the cystic degeneration of solid tumors, such as thick, irregular walls, multiple thick septa within the cyst, and the presence of a distinct solid component in a cystic lesion. Cystic degeneration of solid tumors must be differentiated from other benign cystic lesions because malignant tumors can also undergo cystic degeneration.

Gastrointestinal Stromal Tumor

Gastrointestinal stromal tumors (GISTs) are the most common mesenchymal tumors of the GI tract. They are most frequently found in the stomach, followed by the small bowel, duodenum, colon, rectum, and esophagus (11). GISTs are now thought to arise from the interstitial cells of Cajal and can be identified using immunohistochemistry to determine the expression of KIT (CD117), a cell membrane receptor with tyrosine kinase activity (16). Grossly, GISTs appear as well-circumscribed, lobulated, fleshy masses. GISTs can potentially demonstrate heterogeneous appearances due to areas of hemorrhage, necrosis, and cystic degeneration in the cut section. Histologic features of GISTs can be classified into three patterns: predominant presence of spindle cells (most common)

(Fig. 6), predominant presence of epithelioid cells, or an admixture of spindle and epithelioid elements (16). Immunohistochemically, most tumors are positive for CD117. The most widely accepted criteria for evaluating the biologic behavior of GISTs (very low, low, intermediate, or high risk) are based on the combination of tumor size and mitotic activity. If the tumor is > 5 cm and the mitotic activity is > 5 mitoses for every 50 high-power fields, the lesion can be classified as demonstrating a high risk of aggressive behavior (16).

The radiologic features of GISTs can vary depending on the size and level of aggressive behavior of the tumor. GISTs can appear as round, well-defined, homogeneous submucosal masses with contrast enhancement on CT and MRI if necrosis, hemorrhage, and cystic degeneration are not present. Some GISTs can show a cystic appearance resulting from central hemorrhage and necrosis. Cystic change is detected even when the tumor is small (Fig. 6). GISTs rarely manifest as a multilocular cystic mass (Fig. 7). A CT scan reveals a unilocular or multilocular thick-walled cystic mass with a peripheral enhancement pattern adjacent to the GI tract (Fig. 7). The low attenuation in the center of these lesions corresponds to hemorrhage or necrosis. MR imaging features of GISTs vary depending on the degree of necrosis and hemorrhage. Solid tumor portions yield low signal intensity on T1-weighted images, high signal intensity on T2-weighted images, and enhancement after gadolinium administration upon dynamic examination. Areas of hemorrhage within the tumor vary from a high-to-low signal intensity on both T1- and T2-weighted images (17).

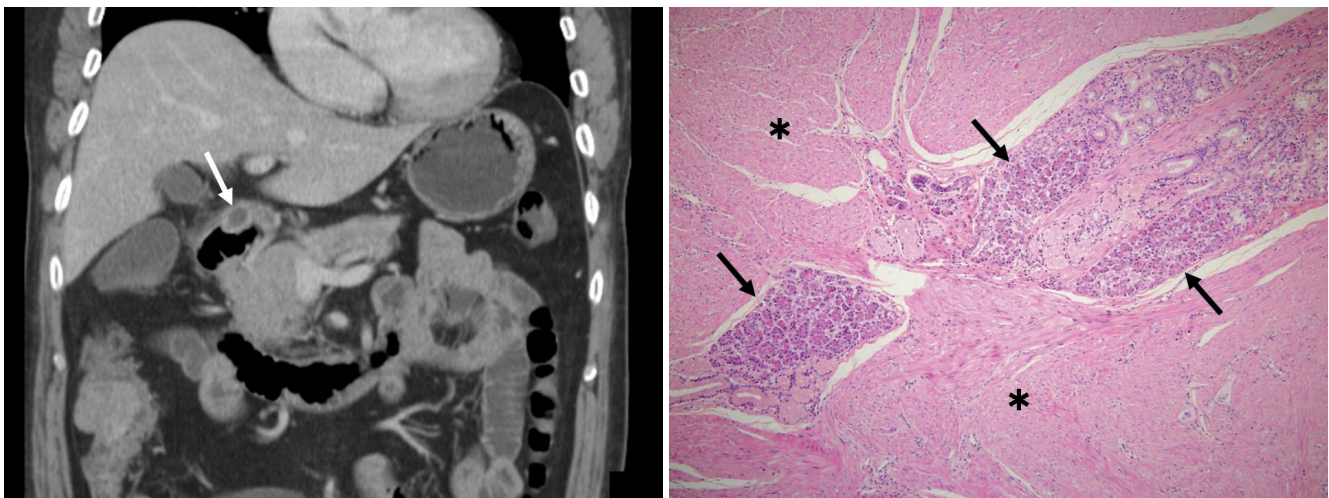


Fig. 3. Heterotopic pancreas in 57-year-old man with cecal cancer. **A.** Contrast-enhanced CT scan shows small cystic lesion (arrow) in gastric antrum. **B.** Photomicrograph shows heterotopic pancreatic acini islands (arrows) in smooth muscle layer of stomach (asterisks; Hematoxylin & Eosin stain, ×100).

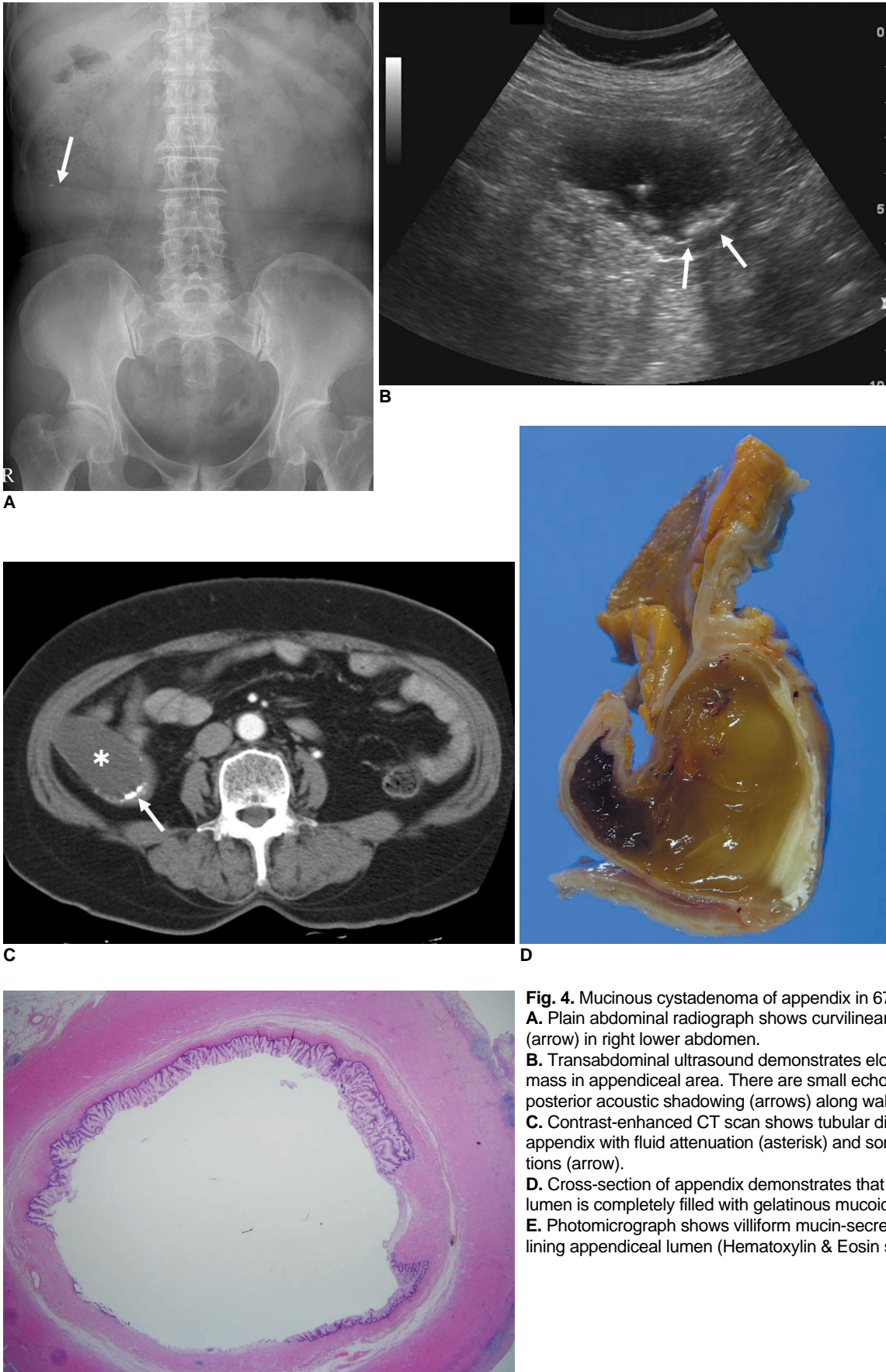
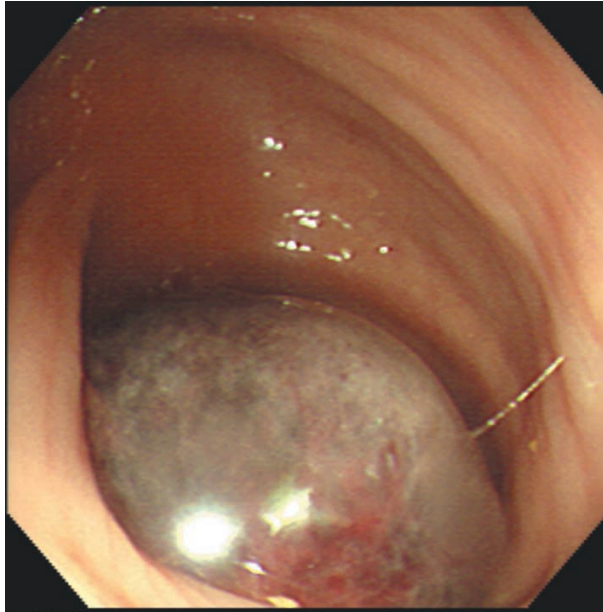
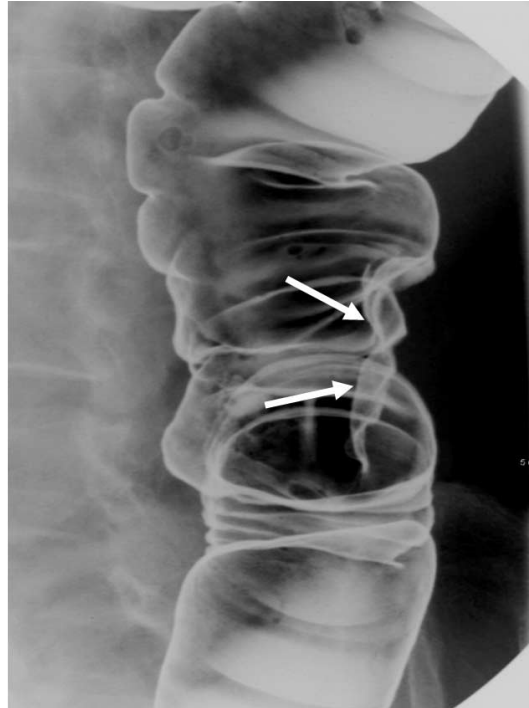


Fig. 4. Mucinous cystadenoma of appendix in 67-year-old man. **A.** Plain abdominal radiograph shows curvilinear calcifications (arrow) in right lower abdomen. **B.** Transabdominal ultrasound demonstrates elongated cystic mass in appendiceal area. There are small echogenic lesions with posterior acoustic shadowing (arrows) along wall of appendix. **C.** Contrast-enhanced CT scan shows tubular dilatation of appendix with fluid attenuation (asterisk) and some wall calcifications (arrow). **D.** Cross-section of appendix demonstrates that appendiceal lumen is completely filled with gelatinous mucoid material. **E.** Photomicrograph shows villiform mucin-secreting epithelium lining appendiceal lumen (Hematoxylin & Eosin stain, $\times 12.5$).

Cystic Lesions of GI Tract



A



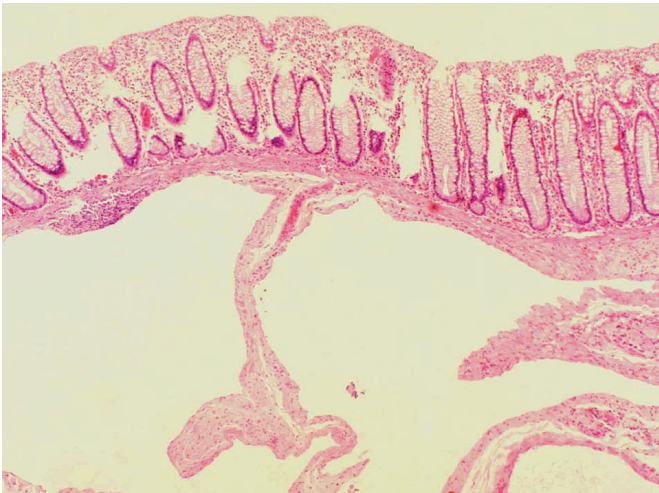
B



C



D



E

Fig. 5. Cystic lymphangioma in colon of 57-year-old man.
A. Endoscopy shows blue-tinged, submucosal mass with smooth surface in descending colon.
B. Barium study demonstrates smooth-surfaced polypoid mass (arrows) in lateral wall of descending colon.
C. Contrast-enhanced CT scan shows multiseptate cystic mass (arrows) in descending colon.
D. Cut surface of gross specimen reveals septated cystic mass with clear fluid in submucosal layer of descending colon.
E. Photomicrograph shows variable-sized, thin-walled cystic spaces lined with flattened endothelial cells (Hematoxylin & Eosin stain, $\times 40$).

Schwannoma

Gastrintestinal schwannomas, or neurilemmomas, account for 2–6% of all GI mesenchymal tumors (11). GI schwannomas arise from the myenteric plexus and are located in the submucosa and muscularis propria of the digestive tract wall. GI schwannomas have a predilection for the stomach (60–70% of cases), followed by the colon and rectum (18, 19). On gross evaluation, GI schwannomas appear to be well-encapsulated; however, histologically, GI schwannomas interdigitate with the surrounding stroma as S100-positive spindle cells admixed with a loose myxoid stroma (Fig. 8). The tumor cells may also form compact

fascicles with weak nuclear palisading. GI schwannomas have some distinctive histologic features, including peripheral lymphoid cuffs with germinal centers (Fig. 8), a lack of hyalinized blood vessels, or a fibrous capsule (20). In contrast with conventional soft tissue schwannomas, secondary degenerative changes, such as central necrosis, hemorrhage, and hyalinization, are rarely present (19, 20). GI schwannomas are usually detected as incidental findings; however, they can present with symptoms of dysphagia, intestinal obstruction, or GI bleeding (18–20).

Transabdominal US reveals a well-defined mass with homogenous internal echogenicity lower than that of

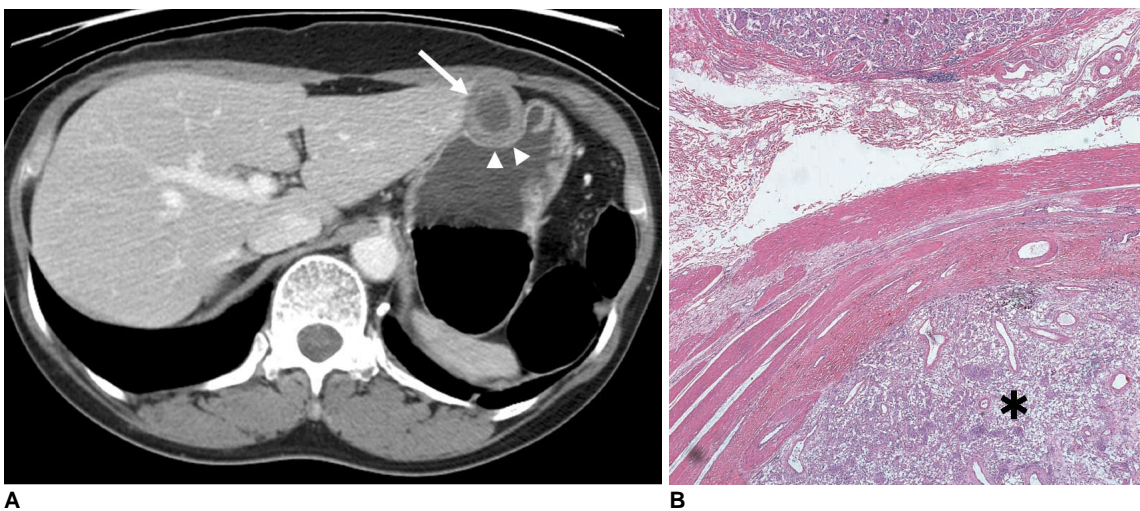


Fig. 6. Gastric gastrointestinal stromal tumor with cystic changes in 58-year-old woman.
A. Contrast-enhanced CT scan shows well-defined cystic mass (arrow) in anterior wall of gastric body. Mass appears to have homogeneous low attenuation with thick, enhancing rim. Note intact overlying gastric mucosa (arrowheads).
B. Photomicrograph shows mass composed of spindle cells (asterisk) in muscular layer of stomach (Hematoxylin & Eosin stain, × 40).

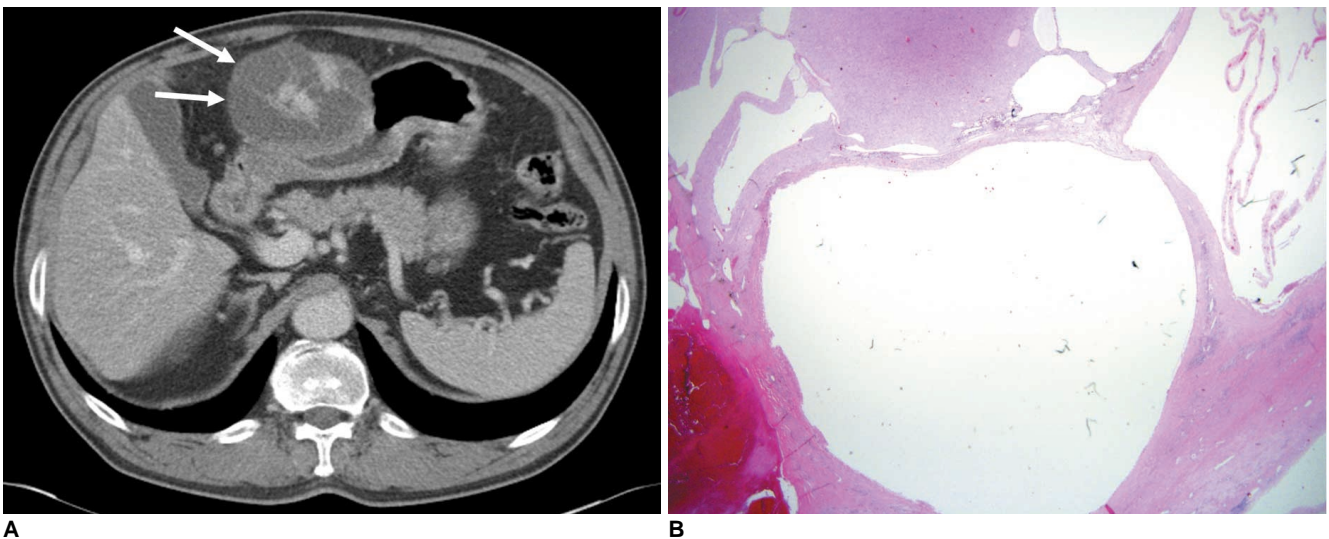


Fig. 7. Gastric gastrointestinal stromal tumor with hemorrhage in 71-year-old man.
A. Contrast-enhanced CT scan shows multilocular cystic mass (arrows) in anterior wall of gastric antrum.
B. Photomicrograph shows multiple large cystic spaces in mass composed of spindle cells (Hematoxylin & Eosin stain, × 12.5).

Cystic Lesions of GI Tract

normal muscularis propria. Some blood flow can be demonstrated in the mass on color Doppler US (21). On CT, GI schwannomas appear as well-demarcated round or oval, homogeneous masses (Fig. 8) with diverse growth patterns (intraluminal, extraluminal, or both). Moreover, GI schwannomas may enhance over time, with peak enhancement occurring during the equilibrium phase (18).

MISCELLANEOUS LESIONS

Gastritis Cystica Profunda

Gastritis cystica profunda (GCP) is an ectopic proliferation of gastric glandular elements, typically located beneath a normal mucosal layer. GCP is a rare submucosal lesion that is often reported in the setting of a prior gastroenterostomy (22). However, it can occasionally be found in the stomach without previous surgery, in which case it is often related to chronic gastritis or ischemia. Histologically, the lesion extends into the gastric

submucosal layer and is composed of elongated hyperplastic gastric foveolae with hyperplasia and cystic dilation of the gastric glands (Fig. 9). This lesion presents as giant gastric folds, a submucosal tumor (Fig. 9), or an isolated polyp (gastritis cystica polyposa). Although commonly an incidental finding, GCP has been reported to be the cause of abdominal pain, bloating, gastric obstruction, and GI hemorrhage (23).

Only a few reports exist describing the imaging characteristics of GCP. The contrast-enhanced CT findings include a homogeneously enhancing polypoid lesion or heterogeneously-enhancing gastric wall thickening, with or without small cystic components (24) (Fig. 9).

Brunner's Gland Hyperplasia

Brunner's glands consist of mucin-secreting glands that are normally located in the deep mucosa and submucosa of the duodenum. These glands protect the duodenal mucosa from the damaging effects of gastric acid. In addition, they

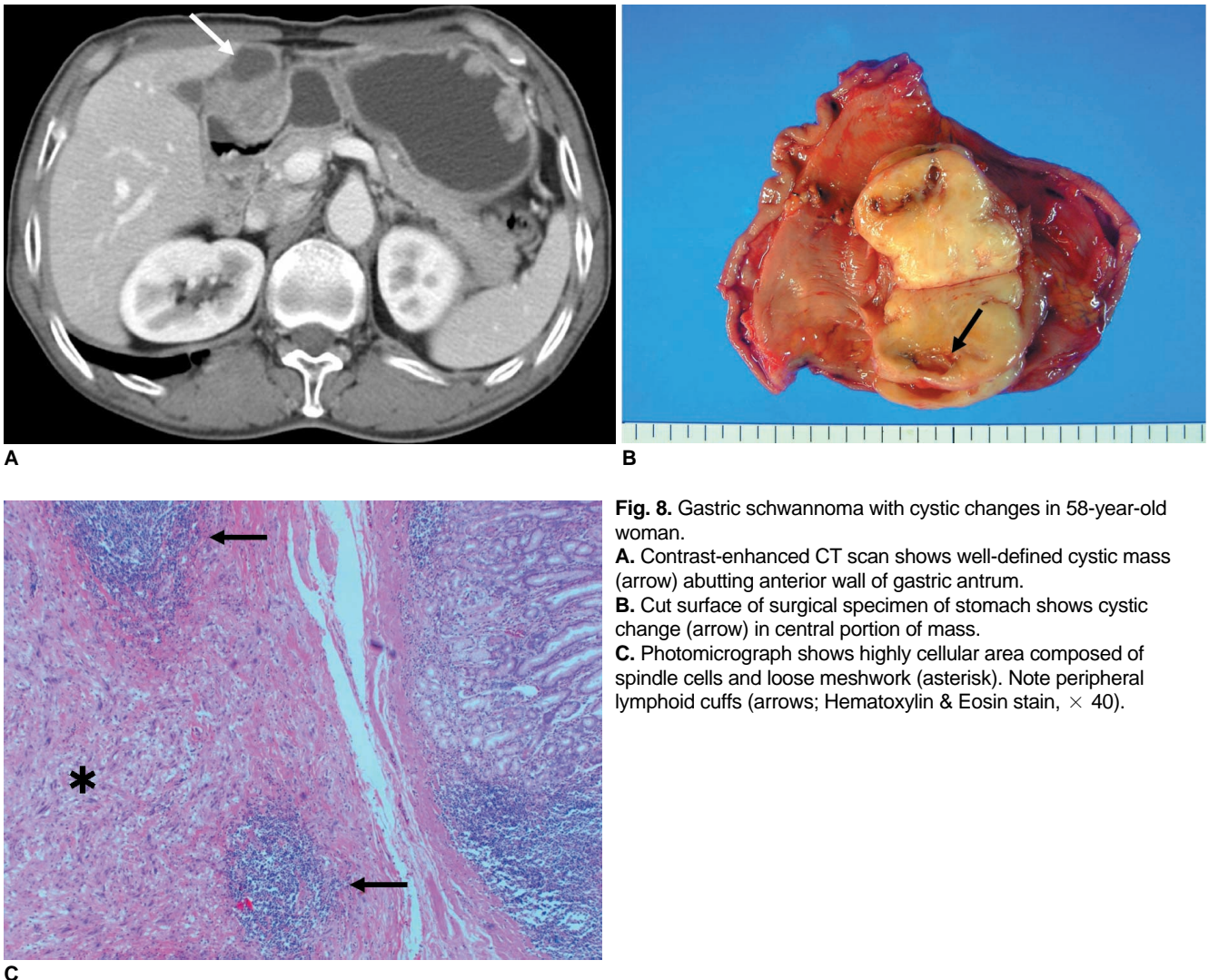
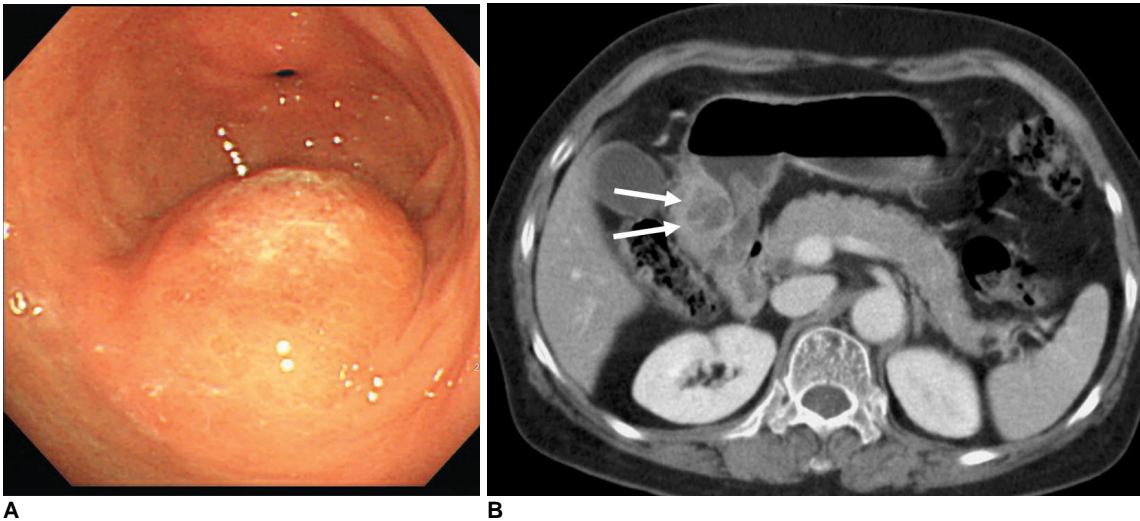


Fig. 8. Gastric schwannoma with cystic changes in 58-year-old woman.

A. Contrast-enhanced CT scan shows well-defined cystic mass (arrow) abutting anterior wall of gastric antrum.

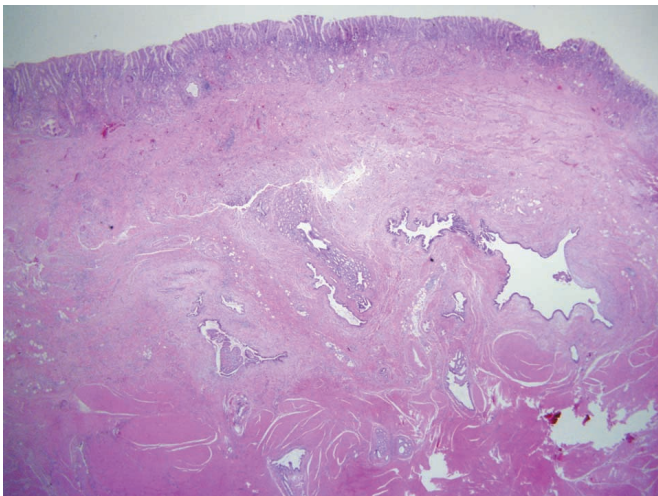
B. Cut surface of surgical specimen of stomach shows cystic change (arrow) in central portion of mass.

C. Photomicrograph shows highly cellular area composed of spindle cells and loose meshwork (asterisk). Note peripheral lymphoid cuffs (arrows; Hematoxylin & Eosin stain, $\times 40$).



A

B



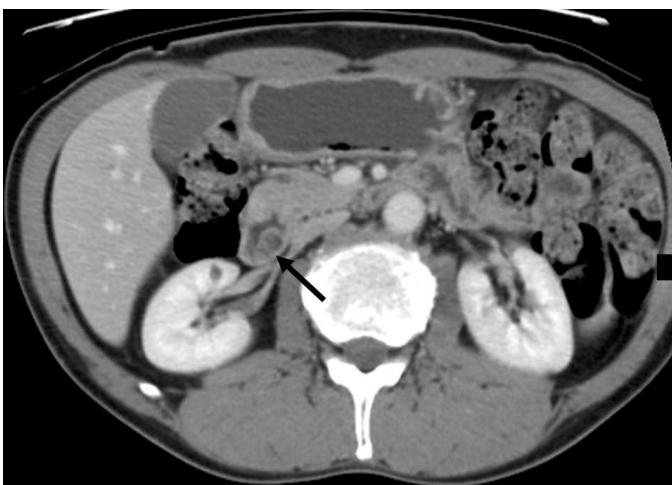
C

Fig. 9. Gastritis cystica profunda in 61-year-old woman.

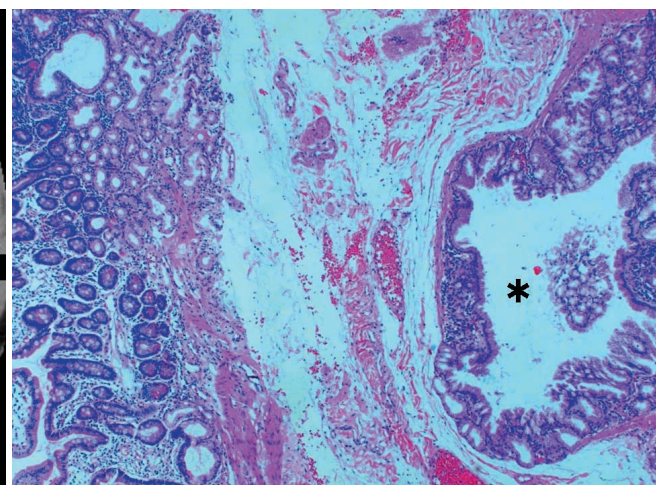
A. Endoscopy shows polypoid lesion with smooth surface and patches of erythema, but no erosions. Surrounding mucosa appears normal.

B. Contrast-enhanced CT scan shows polypoid cystic mass in gastric antrum (arrows).

C. Photomicrograph shows cystic dilatation of heterotopic gastric glands in submucosal and muscular layers (Hematoxylin & Eosin stain, $\times 12.5$).



A



B

Fig. 10. Brunner's gland hyperplasia in 48-year-old man.

A. Contrast-enhanced CT scan shows cystic mass (arrow) in second section of duodenum.

B. Photomicrograph demonstrates cystic changes of hyperplastic Brunner's glands (asterisk) with lobular architecture in submucosa (Hematoxylin & Eosin stain, $\times 40$).

extend from the pylorus to the second portion of the duodenum, up to the papilla, and may, in rare cases, extend to the proximal jejunum (25). Histologically, Brunner's gland hyperplasia may manifest as solitary or multiple small nodules composed of proliferating glands with maintenance of a lobular architecture and fibrous septa separating the hyperplastic lobules (Fig. 10). They can show a cystic appearance because of the dilatation of the glandular acini or ducts. Brunner's gland hyperplasia is clinically important because it can be mistaken for neoplastic lesions, although it is usually asymptomatic.

A barium study indicates that Brunner's gland hyperplasia commonly appears as smooth, polypoid lesions of the duodenum and may show markedly thickened, irregular folds in the proximal duodenum because of concomitant duodenitis (26). Moreover, Brunner's gland hyperplasia may be detected on transabdominal US as a lesion with a heterogeneous echotexture because of multiple small cysts (27). Only a few reports have described the various CT findings of Brunner's gland hyperplasia, including findings of a homogeneously-enhancing mass or of a heterogeneous and hypoattenuating mass with contrast administration (28, 29). In our study, CT revealed a solitary cystic lesion with mild wall enhancement (Fig. 10), which correlates with cystic dilatation of Brunner's glands.

CONCLUSION

Diagnosis of cystic lesions of the GI tract is difficult because of non-specific clinical manifestations and radiologic features. The clinical features of these lesions vary depending on the size and location of the lesion and they usually appear as a submucosal mass upon radiologic examinations. Despite the overlap of the radiologic appearance of various GI cystic lesions, the anatomic location and certain radiologic details of the lesion can help narrow the differential diagnosis. Finally, it is important for radiologists to be familiar with various disease categories and imaging characteristics of cystic lesions of the GI tract in order to facilitate the accurate diagnosis and proper management of such lesions.

References

- Macpherson RI. Gastrointestinal tract duplications: clinical, pathologic, etiologic, and radiologic considerations. *Radiographics* 1993;13:1063-1080
- Bower RJ, Sieber WK, Kiesewetter WB. Alimentary tract duplications in children. *Ann Surg* 1978;188:669-674
- Theodosopoulos T, Marinis A, Karapanos K, Vassilikostas G, Dafnios N, Samanides L, et al. Foregut duplication cysts of the stomach with respiratory epithelium. *World J Gastroenterol* 2007;13:1279-1281
- Kangaroo H, Sample WF, Hansen G, Robinson JS, Sarti D. Ultrasonic evaluation of abdominal gastrointestinal tract duplication in children. *Radiology* 1979;131:191-194
- Wang C, Kuo Y, Yeung K, Wu C, Liu G. CT appearance of ectopic pancreas: a case report. *Abdom Imaging* 1998;23:332-333
- Levine MS. *Benign tumors of the stomach and duodenum*. In: Gore RM, Levine MS, eds. *Textbook of gastrointestinal radiology*, 3rd ed. Philadelphia, PA: Saunders Elsevier, 2008:593-617
- Cho JS, Shin KS, Kwon ST, Kim JW, Song CJ, Noh SM, et al. Heterotopic pancreas in the stomach: CT findings. *Radiology* 2000;217:139-144
- Lopez-Pelaez MS, Hoyos FB, Isidro MG, Unzurrunzaga EA, Lopez Ede V, Collazo YQ. Cystic dystrophy of heterotopic pancreas in stomach: radiologic and pathologic correlation. *Abdom Imaging* 2008;33:391-394
- Park SH, Han JK, Choi BI, Kim M, Kim YI, Yeon KM, et al. Heterotopic pancreas of the stomach: CT findings correlated with pathologic findings in six patients. *Abdom Imaging* 2000;25:119-123
- Dachman AH, Lichtenstein JE, Friedman AC. Mucocele of the appendix and pseudomyxoma peritonei. *AJR Am J Roentgenol* 1985;144:923-929
- Fenoglio-Preiser CM. *Gastrointestinal pathology: an atlas and text*, 3rd ed. Philadelphia: Wolters Kluwer/Lippincott Williams & Wilkins, 2008
- Pickhardt PJ, Levy AD, Rohrmann CA Jr, Kende AI. Primary neoplasms of the appendix: radiologic spectrum of disease with pathologic correlation. *Radiographics* 2003;23:645-662
- Sasaki K, Ishida H, Komatsuda T, Suzuki T, Konno K, Ohtaka M, et al. Appendiceal mucocele: sonographic findings. *Abdom Imaging* 2003;28:15-18
- Zhu H, Wu ZY, Lin XZ, Shi B, Upadhyaya M, Chen K. Gastrointestinal tract lymphangiomas: findings at CT and endoscopic imaging with histopathologic correlation. *Abdom Imaging* 2008;33:662-668
- Agha FP, Francis IR, Simms SM. Cystic lymphangioma of the colon. *AJR Am J Roentgenol* 1983;141:709-710
- Fletcher CD, Berman JJ, Corless C, Gorstein F, Lasota J, Longley BJ, et al. Diagnosis of gastrointestinal stromal tumors: a consensus approach. *Hum Pathol* 2002;33:459-465
- Levy AD, Remotti HE, Thompson WM, Sobin LH, Miettinen M. Gastrointestinal stromal tumors: radiologic features with pathologic correlation. *Radiographics* 2003;23:283-304
- Levy AD, Quiles AM, Miettinen M, Sobin LH. Gastrointestinal schwannomas: CT features with clinicopathologic correlation. *AJR Am J Roentgenol* 2005;184:797-802
- Hou YY, Tan YS, Xu JF, Wang XN, Lu SH, Ji Y, et al. Schwannoma of the gastrointestinal tract: a clinicopathological, immunohistochemical and ultrastructural study of 33 cases. *Histopathology* 2006;48:536-545
- Miettinen M, Shekitka KM, Sobin LH. Schwannomas in the colon and rectum: a clinicopathologic and immunohistochemical study of 20 cases. *Am J Surg Pathol* 2001;25:846-855
- Fujii Y, Taniguchi N, Hosoya Y, Yoshizawa K, Yasuda Y, Nagai H, et al. Gastric schwannoma: sonographic findings. *J Ultrasound Med* 2004;23:1527-1530
- Franzin G, Novelli P. Gastritis cystica profunda. *Histopathology* 1981;5:535-547
- Kurland J, DuBois S, Behling C, Savides T. Severe upper-GI bleed caused by gastritis cystica profunda. *Gastrointest Endosc* 2006;63:716-717

24. Wu MT, Pan HB, Lai PH, Chang JM, Tsai SH, Wu CW. CT of gastritis cystica polyposa. *Abdom Imaging* 1994;19:8-10
25. Giacosa A. Morphometry of normal duodenal mucosa. *Scand J Gastroenterol Suppl* 1989;167:10-12
26. Levine MS. *Benign tumors of the stomach and duodenum*. In: Gore RM, Levine MS, eds. *Textbook of gastrointestinal radiology*, 3rd ed. Philadelphia, PA: Saunders Elsevier, 2008:593-617
27. Patel ND, Levy AD, Mehrotra AK, Sobin LH. Brunner's gland hyperplasia and hamartoma: imaging features with clinicopathologic correlation. *AJR Am J Roentgenol* 2006;187:715-722
28. Stolpman DR, Hunt GC, Sheppard B, Huang H, Gopal DV. Brunner's gland hamartoma: a rare cause of gastrointestinal bleeding -- case report and review of the literature. *Can J Gastroenterol* 2002;16:309-313
29. Block KP, Frick TJ, Warner TF. Gastrointestinal bleeding from a Brunner's gland hamartoma: characterization by endoscopy, computed tomography, and endoscopic ultrasound. *Am J Gastroenterol* 2000;95:1581-1583